LAWRENCE
LIVERMORE
NATIONAL
LABORATORY

LLNL-TR-400974

Shell Element Verification & Regression Problems for DYNA3D

Edward Zywicz
Methods Development Group

January 31, 2008

This document was prepared as an account of work sponsored by an agency of the United States government. Neither the United States government nor Lawrence Livermore National Security, LLC, nor any of their employees makes any warranty, expressed or implied, or assumes any legal liability or responsibility for the accuracy, completeness, or usefulness of any information, apparatus, product, or process disclosed, or represents that its use would not infringe privately owned rights. Reference herein to any specific commercial product, process, or service by trade name, trademark, manufacturer, or otherwise does not necessarily constitute or imply its endorsement, recommendation, or favoring by the United States government or Lawrence Livermore National Security, LLC. The views and opinions of authors expressed herein do not necessarily state or reflect those of the United States government or Lawrence Livermore National Security, LLC, and shall not be used for advertising or product endorsement purposes.

This work performed under the auspices of the U.S. Department of Energy by Lawrence Livermore National Laboratory under Contract DE-AC52-07NA27344.

Shell Element Verification & Regression Problems for DYNA3D

Edward Zywicz
Methods Development Group
Defense Technologies Engineering Division
Engineering Directorate

January 31, 2008

Abstract

A series of quasi-static regression/verification problems were developed for the triangular and quadrilateral shell element formulations contained in Lawrence Livermore National Laboratory's explicit finite element program DYNA3D. Each regression problem imposes both displacement- and force-type boundary conditions to probe the five independent nodal degrees of freedom employed in the targeted formulation. When applicable, the finite element results are compared with small-strain linear-elastic closed-form reference solutions to verify select aspects of the formulations' implementation. Although all problems in the suite depict the same geometry, material behavior, and loading conditions, each problem represents a unique combination of shell formulation, stabilization method, and integration rule. Collectively, the thirty-six new regression problems in the test suite cover nine different shell formulations, three hourglass stabilization methods, and three families of through-thickness integration rules.

1 INTRODUCTION

DYNA3D is an explicit finite element code written at Lawrence Livermore National Laboratory (Lin, 2005). As described by its originator, it is used to simulate "*dyna*mics in *three-dimensions*" - hence its name. DYNA3D contains a variety of discrete, solid, and structural elements. The present effort aims to verify aspects of the implementation of DYNA3D's shell element formulations and generate a series of problems suitable for incorporation into DYNA3D's regression test suite.

The verification approach adopted herein contains several conceptual steps. First, a series of simple boundary value problems are developed for which analytical solutions exist. The problems consist of a long cantilevered rectangular beam loaded in a variety of ways. Next, finite element (FE) models are assembled for each problem, and DYNA3D is used

to simulate the mechanical response. The numerical results are checked against themselves for orientation dependence and each other for consistency and compared to reference solutions. The series of boundary value problems are reproduced in several different orientations and bundled into a single FE input deck. An input deck is assembled for each shell element variant explored, i.e., formulation, through-thickness integration rule, stabilization method, etc. To assist in the verification process, post-processing tools are developed to automatically extract the desired comparison metrics and check for orientation independence.

The verification/regression problems described here represent a balance between two goals. Each of the shell's five nodal degrees of freedom (DOF) is individually probed using both imposed displacement/rotation and force/moment boundary conditions. This allows the element kinematics and element reaction forces to be examined. Unfortunately, this required that some FE models employ boundary conditions that differ from their corresponding classic boundary value problem, and hence not all problems have reference solutions to compare against. Also, the FE models use just enough elements to capture the basic response, but not always enough elements to be fully converged and yield the reference solution. Nonetheless, the overall verification goal is achieved and the desire to develop a set of practical shell element regression problems is satisfied.

In section 2, the report summarizes DYNA3D's different shell element formulations along with their integration schemes, stabilization methods and other available variants. Section 3 describes the attributes of a generic beam and incorporates this beam into a series of boundary value problems by subjecting it to a variety of different boundary conditions. Analytical solutions for each unique boundary value problem are presented. In section 4 the FE models are presented, and in section 5 a discussion is given of how the FE model results are anticipated to compare with their reference solutions. Section 6 presents the numerically generated results and compares them to their reference solutions.

2 DYNA3D'S SHELL FORMULATIONS

DYNA3D presently contains nine different shell element formulations of which seven are quadrilateral geometries and two are triangular geometries. The quadrilateral shell formulations are:

- Bathe-Dvorkin (*BD*)
- Belytschko-Lin-Tsay (*BLT*)
- Belytschko-Lin-Tsay (*BLTr*) - selective-reduced integration
- Hughes-Liu (*HL*)
- Membrane (*Mem*)
- YASE (*Y*)
- YASE (*Y4*) – fully integrated

and the triangular formulations are:

- Bazeley-Cheung-Irons-Zienkiewicz (*BCIZ*)

- Belytschko-Matchertas (*C0*)

All the formulations, except the membrane, utilize five DOF per node. The remaining DOF, commonly referred to as the "drill" DOF, represents the rotation about a vector that is approximately normal to the reference shell surface, and in these formulations this DOF does not contribute to the element kinematics.

The Hughes-Liu, Belytschko-Lin-Tsay, membrane, and YASE formulations use one in-plane integration point while the remaining formulations employ three or four. With the exception of the YASE element, which is physically stabilized, all of DYNA3D's one-point shell formulations require some form of hourglass stabilization to suppress zero energy modes. The three hourglass control methods available in DYNA3D are:

- Viscous based (*v*)
- Stiffness based (*s*)
- Combination of viscous and stiffness based (*c*)

The viscous method applies hourglass control forces whose values depend upon a viscosity and the rate the element is deforming in a particular hourglass mode. This form of stabilization has no memory and is completely dissipative. Stiffness based hourglass control differs from viscous in that its forces are based upon a material stiffness and, in an incremental manner, the total amount an element has deformed in each of its hourglass modes. Although in theory this method conserves energy, in application it is subject to various non-linear effects. The last scheme is just a combination of the two basic methods and is implemented in DYNA3D by applying both methods simultaneously, but with reduced viscosity (5%) and stiffness (95%) values.

DYNA3D employs numerical integration to integrate the through-thickness response of its shell elements - except when the resultant shell element material model is used. There are three integration methods available:

- User-defined numerical integration (*u*)
- Gauss quadrature integration (*g*)
- Trapezoidal integration (*t*)

Any non-zero number of integration points can be used with user-defined and trapezoidal rules, while Gauss quadrature can use between one and five integration points. Although the trapezoidal rule locates integration points on both the upper and lower shell faces, making the surface stresses and strains directly available for post-processing, it is less accurate than Gauss quadrature.

Lastly, the Hughes-Liu shell formulation differs from the other formulations in that the location of the reference surface is user selected. The reference surface can be located at the top, the middle, or the bottom of element. By default the reference surface is located in the middle.

3 THE GENERIC BEAM

The fundamental structure used for testing in this work is a cantilevered rectangular beam. This simple structure can be loaded in a variety of ways and allows comparisons between readily available reference solutions and numerical simulations. This section describes the generic beam, how it is loaded, and its predicted responses.

3.1 PHYSICAL DESCRIPTION

Shown schematically in Figure 1 is the generic cantilevered beam used in this work. The length of the beam, L = 0.15 m, is three times its width, w = 0.05 m, and thirty times is height, h = 0.005 m. The beam material is specified as linear elastic with a Young's modulus (E) of 200 GPa, a Poisson's ratio of 0.3, and a density of 7860 kg/m^3. The beam is aligned with a local *i*-*j*-*k* coordinate system such that its length runs in the positive *i*-direction and its width runs in the *j*-direction. The left end of the beam, labeled A, is fixed, i.e., all of its displacements and rotations are constrained. The free end of the beam, labeled B, is loaded by a single displacement or force in the *i*-, *j*-, or *k*-direction, or by a single rotation or moment about the *i* or *j* axis.

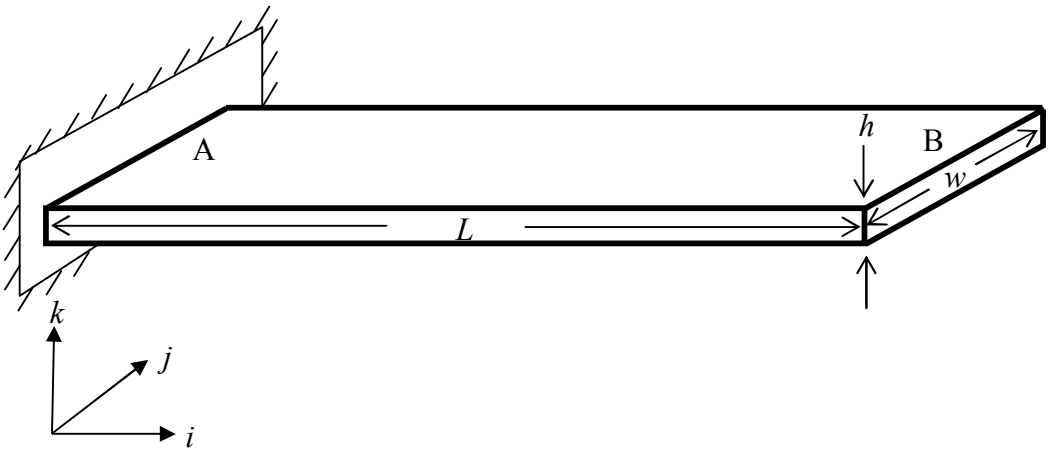

Figure 1. *Generic beam geometry*

3.2 THEORETICAL RESPONSES TO IMPOSED LOADINGS

The generic beam can respond in a variety of ways depending upon the boundary condition imposes on its free end B. Define I_j and I_k as the moment of inertia about the *j*- and *k*-axes, respectively, as

$$I_j = \frac{wh^3}{12} \qquad (2)$$

$$I_k = \frac{hw^3}{12} \tag{3}$$

and let A_c denote the cross sectional area hw. Table 1 contains reference solutions for the translational displacement u and rotation ϕ of the beam's free-end when a force F is applied in the i-, j-, or k-direction (load cases 1 to 3) or a moment M (load cases 4 and 5) is applied about the i or j axis at B (Beer and Johnston, 1981; Rathbun, 2007). Provided that the imposed loads and moments are sufficiently small, i.e., consistent with the linearized theory employed, the remaining translations and rotations are approximately zero. Note that since the reference solutions are based upon traditional beam theory, shear deformation is neglected. Table 2 contains expressions for the reaction forces and moments at end A when a displacement (load cases 6 to 8) or rotation (load cases 9 and 10) is applied at end B as well as relations for the unspecified translation or rotation at end B (Beer and Johnston, 1981; Rathbun, 2007).

Table 1: *Applied Force/Moment, Boundary Conditions and Reference Solutions. Magnitudes of the imposed loads for numerical tests are shown in parentheses.*

Load Case Number	Applied Force/Moment at End B	End B Translation	End B Rotation
1	F_i (5000 Nt)	$u_i = \frac{F_i L}{A_c E}$	$\phi_k = 0$
2	F_j (0.2 Nt)	$u_j = \frac{F_j L^3}{3EI_k}$	$\phi_k = \frac{F_j L^2}{2EI_k}$
3	F_k (100 Nt)	$u_k = \frac{F_k L^3}{3EI_j}$	$\phi_j = \frac{F_k L^2}{2EI_j}$
4	M_i (0.1 Nt-m)	$u_{j,k} = 0$	$\phi_i = \frac{M_i L}{J_i G}$ $J_i = wh^3[\frac{16}{3} - 3.36\frac{h}{w}(1 - \frac{h^4}{12w^4})]$ *
5	M_j (50 Nt-m)	$u_k = \frac{M_j L^2}{2EI_j}$	$\phi_j = \frac{M_j L}{EI_j}$

* - Reference (Young, 1989)

Table 2: *Applied Translation/Rotation, Boundary Conditions and Reference Solutions. Magnitudes of the imposed deformations for numerical tests are shown in parentheses.*

Load Case Number	Applied Translation / Rotation at End B	Reaction at End A	End B Rotation / Translation
6	u_i ($1.5\text{x}10^{-5}$ m)	$F_i = \frac{A_c E}{L} u_i$	*0*
7	u_j ($5\text{x}10^{-3}$ m)	$F_j = \frac{3EI_k}{L^3} u_j$, $M_k = \frac{3EI_k}{L^2} u_j$	$\phi_k = \frac{3}{2L} u_j$
8	u_k ($1\text{x}10^{-3}$ m)	$F_k = \frac{3EI_j}{L^3} u_k$, $M_j = \frac{3EI_j}{L^2} u_k$	$\phi_j = \frac{3}{2L} u_k$
9	ϕ_i (0.1 rad)	$M_i = \frac{J_i G}{L} \phi_i$	*0*
10	ϕ_j (0.1 rad)	$M_j = \frac{EI_j}{L} \phi_j$	$u_k = \frac{L}{2} \phi_j$

Besides the ten loadings depicted in Tables 1 and 2, rotational boundary conditions could also be applied in the *k*-direction at the tip B. These loadings are excluded since they would result in applying boundary conditions to the drill DOF.

4 FINITE ELEMENT MODEL

4.1 THE BASIC FINITE ELEMENT MODEL

Three square shell elements are used to simulate each beam modeled. For triangular formulations, each quadrilateral shell is replaced with two triangular ones. Although finer meshes were tried and yielded better agreement with the reference solutions, the present discretization ran the fastest and yielded results, as will be shown later, that differ by less than 6% from the reference values for quadrilateral formulations.

To probe each of the beam's DOF under displacement- and force-type boundary conditions, a collection of ten independent beams are modeled and each is loaded with one of the loadings represented in Tables 1 and 2. Within each test case (i.e., a single DYNA3D input deck), three groups of tens beams are included. Each group has its beams' *i*-axis aligned with a different global *X*-*Y*-*Z* coordinate axis to verify that the software implementation is truly independent of the global coordinate system. Consequently, each test case (i.e., input deck) models thirty beams using ninety shell elements.

The application of displacement- and force-type boundary conditions is imposed using DYNA3D's *Prescribed Velocity and Acceleration* and *Nodal Forces and Follower Forces* options, respectively. The magnitude of the boundary condition is increased linearly in time from zero to its full value over 0.1 seconds and then held constant as schematically depicted in Figure 2. The total displacement, rotation, force or moment

imposed on the B end beam nodes are included in Tables 1 and 2 for each of the ten loading cases examined. The magnitudes of the imposed loads are shown in parentheses right after the loading variable. In the case of force or moment boundary conditions, the load magnitude is distributed equally to both end nodes.

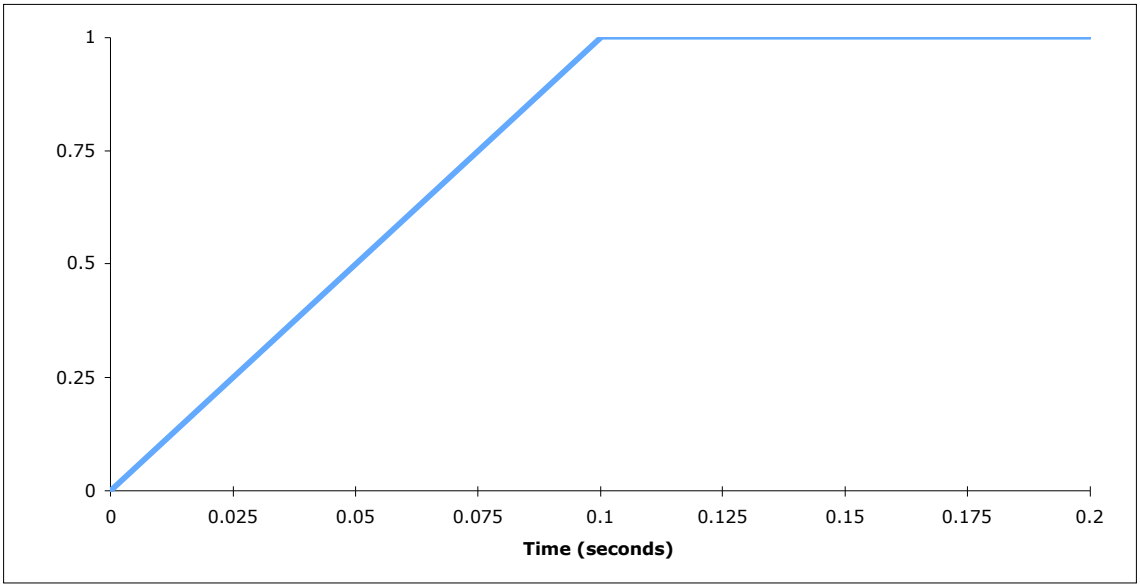

Figure 2. *Load curve time history*

It was observed that out-of-plane displacements sometimes occurred when the beam was sheared in the plane (cases 2 and 7), i.e., a shear buckling type deformation. To prevent this, boundary conditions prohibiting out-of-plane displacements were imposed on the tip nodes for cases 2 and 7.

Each simulation is run for 0.2 seconds and uses mass proportional damping to reduce undesirable oscillations in the problem. The fraction of critical damping applied is $\xi = 0.1$ at a frequency of 1000 rad/sec. This combination, obtained via trail and error, reduces the oscillations without compromising the final steady-state solution.

When activated, DYNA3D's *Prescribed Velocity and Acceleration* option can report the reaction forces or moments necessary to achieve the desired boundary condition. This feature is used to quantify the reaction forces and moments on the A end of the beam. When the value of a reaction force or moment is desired on a fixed boundary, a prescribed velocity with a magnitude of zero is applied to the corresponding DOF.

4.2 THE TEST SUITE

To verify that the shell element formulation, hourglass control, through-thickness integration rule, and, as applicable, its reference surface location are functioning correctly, a matrix of test cases using different combinations of the possible variants was assembled. Table 3 lists the variants examined for each shell formulation. Each 1- to 4-

digit group of numbers and letters denotes a single case (i.e., a DYNA3D input deck) and describes the specific combinations considered in it. Here, the number indicates the number of through-thickness integration points, the letter *g (gauss)*, *t (trapezoidal)*, or *u (user-defined)* denotes the integration rule, the letter *v (viscous)*, *s (stiffness)*, *c (combined)* defines the hourglass stabilization method, and the letter *m (minus, i.e., bottom face)* or *p (plus, i.e., top face)* specifies the alternative location of the reference surface. Fortunately, due to the way the shell elements are coded in DYNA3D, it is not necessary to consider every possible combination for every shell formulation to sufficiently test the entire implementation.

Table 3: *Shell Element Variants Tested*

Formulation	# of Through-Thickness Int. Points and Rule, Hourglass Type, & Ref. Surface Location
HL	*2gv, 5tv, 2uv, 2gs, 2gc, 2gvm, 2gvp*
BLT	*2gv, 3gv, 4gv, 5gv, 5tv, 6tv, 2gs, 2gc, 2uv*
Mem	*v, s*
Y	*2g, 5t, 2u*
Y4	*2g, 5t, 2u*
BD	*2g, 5t, 2u*
BLTr	*2g, 5t, 2u*
BCIZ	*2g, 5t, 2u*
C0	*2g, 5t, 2u*

For simplicity and speed, the user-defined integration rule contains only two integration points, and they are located at the two-point Gauss quadrature locations. This simplified the verification process.

5 ANTICIPATED RESULTS

5.1 MODEL INDUCED DIFFERENCES

For the six load cases depicting axial extension (cases 1 and 6) and longitudinal flexure (cases 3, 5, 8, and 12), there exists a direct correspondence between the beam idealizations used to generate the reference solutions and the assembled FE models. In the quadrilateral formulations, the nodal displacements/rotations and the sum of the nodal reaction forces/moments should equal the reference solution values on each end of the generic beam. For triangular formulations, this will also be true, but only when displacement- or rotation-type boundary conditions are imposed. Hence, good agreement between the FE results and the reference solutions should be achieved for these cases.

In the case of in-plane shear loading (cases 2 and 7), limited correlation between the reference solution and FE results is expected. The reference solution, which neglects shear deformation, will be overly stiff since the generic beam has only a three-to-one

length-to-width ratio. The particular boundary conditions used load the elements predominately in an in-plane hourglass mode. This means the FE behavior in the single-point elements will be dictated by the stabilization. Since stiffness stabilization methods only use a small fraction of the stiffness present in a fully integrated element, the FE response will be soft compared to the reference solution. For viscous hourglass control, no steady-state solution will be reached for the load-imposed case (2).

The FE models used in cases 4 and 9 do not represent uni-axial torsion as depicted in the reference solution. The FE model imposes prescribed rotations or moments on the lateral edges at the tip of the beam that shear and bend the cross section. Given the limited length-to-width ratio of the beam, pure torsion will never develop along the beam and agreement between the FE and reference solutions is not anticipated. While a more representative FE model could have been developed for this configuration, it would not have probed this particular nodal DOF.

The reference surface and loadings used in the generic beam problems and FE models coincided for all variants except for the Hughes-Liu models when the reference surface is moved to a face and the membrane problems. In these Hughes-Liu models, the imposed FE boundary conditions differ from those in the generic beam boundary value problems and result in different deformation. Consequently, the reference solutions do not depict the FE loadings and comparisons cannot be made between them. Similarly, the membrane formulation does not utilize rotational DOF and thus membrane elements cannot represent any boundary value problem that requires them.

5.2 THROUGH THICKNESS INTEGRATION

For the small-strain/small-displacement linear-elastic uni-axial extension and longitudinal bending problems considered, two-point Gauss quadrature integrates the through-thickness behavior exactly. Thus, for a given formulation and stabilization combination, the results from the user defined integration rule and all Gauss quadrature rules should be the same.

The trapezoidal rule is not as accurate as Gauss quadrature but does integrate some cases exactly, e.g., the force from uni-axial extension. A convergence study was performed using the Bathe-Dvorkin formulation, the trapezoidal integration rule, and the case where the beam is loaded by a vertical tip force (case 3). Figure 3 shows a single curve that represents the normalized steady-state free-tip vertical displacement and tip rotation as functions of the number of integration points. The displacement and rotation have been normalized by their values calculated using Gauss quadrature. (The normalized results are, for all practical purposes, identical.) Clearly, trapezoidal integration is not as efficient as Gauss quadrature. In this problem, five integration points are required to obtain a relative displacement and rotation of 90% while more than ten points are needed to get a relative value of 98%.

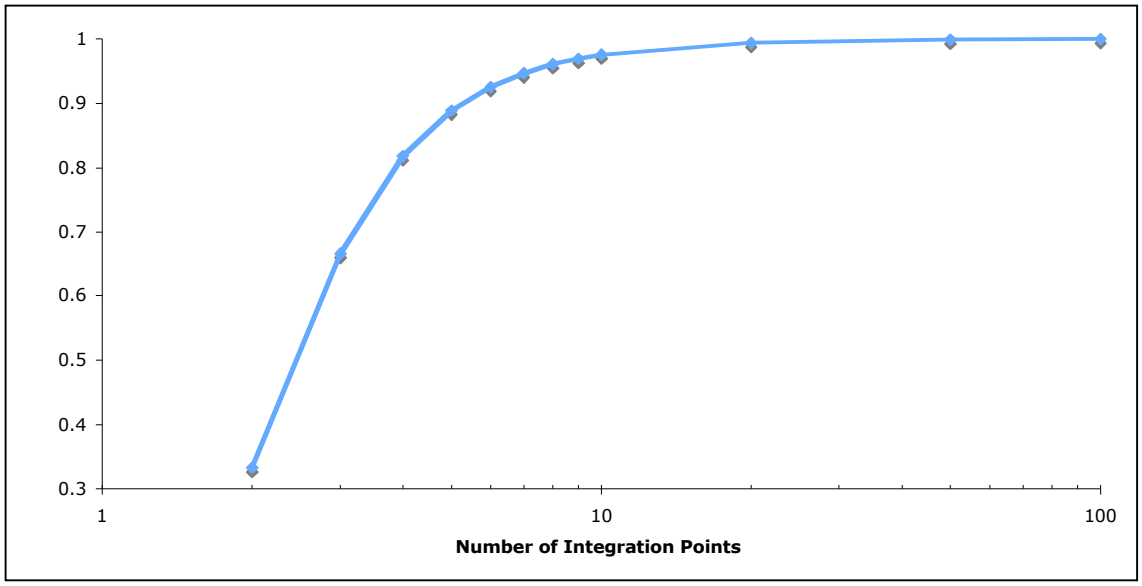

Figure 3. *Normalized tip displacement and rotation vs. number of trapezoidal integration points*

The inherent accuracy of the trapezoidal rule can be evaluated in closed form for select stress distributions. Consider the case of a rectangular beam subjected to pure bending about one if its primary axes. The relative error of the moment is given by

$$e_{mom} = \frac{M_{trap} - M_{exact}}{M_{exact}},$$

where M_{exact} and M_{trap} denote the exact moment and the moment obtained using trapezoidal integration, respectively. Substituting in the appropriate expressions yields

$$e_{mom} = 3\left(\frac{1}{n-1} + \sum_{i=2}^{n-1} \frac{(1-2i+n)^2}{(n-1)^3} \right) - 1,$$

where n is the number of integration points used in the trapezoidal rule. Evaluating e_{mom} for n equal to 5, 10, and 50 gives 1/8, 2/81, and 2/2401, respectively. For $n >> 1$, $e_{mom} > 2/n^2$. In this bending example, trapezoidal integration yields a moment higher than its actual value and has the effect of "stiffening" the response. Hence, in the previous load controlled problem, trapezoidal integration yields tip displacements smaller than the theoretical value.

In the regression test suite, only five points are used with trapezoidal integration. This provides for computationally fast regression problems and results that typically differ by less than 10% from their reference values. However, to ensure that the trapezoidal rule is implemented properly, a series of additional verification runs are made using 50 integration points. The values from these runs should match closely those obtained using Gauss quadrature. Based upon the above expression for e_{mom}, an error of approximately 0.083% is anticipated for bending related variables.

5.3 METRICS FOR EVALUATION

The metrics used for regression testing are the nodal resultant displacements/rotations and forces/moments identified in Tables 1 and 2. These regression metrics, although not fully representative of the underlying boundary value problems, allow the behavior of all FE DOF to be individually examined and continuously monitored. Hence, any modifications that impact the shell formulations should be readily apparent.

The test problem results are checked against themselves and the reference solutions in as many ways as possible to verify the shell formulation implementations. Using all the resultants identified in Tables 1 and 2:

- A consistency check is performed on each variant to ensure that the FE results from the three different orientations all yield the same values when expressed in their local *i-j-k* coordinate system.
- For each shell formulation:
    - The results from all Gauss quadrature and user-defined integration rules are crosschecked for each stabilization method.
    - A run is made using trapezoidal integration with fifty integration points, and its results are compared to those from the two-point Gauss quadrature.

Several additional checks are made using only the quantities from loading cases 1, 3, 5, 6, 8, and 10. For each shell formulation:

- The FE results from each two-point Gauss quadrature run are compared to the reference solution values.
- Variants that differ only in their stabilization method are compared to each other.

In general, little or no difference should exist in any of these comparisons. For obvious reasons, not all of the above checks are made for the membrane formulation and the Hughes-Liu formulation with relocated reference surfaces.

6 RESULTS

The results from each variant are checked at each of their eleven sampling times for orientation independence and visually inspected for any anomalies in their deformed geometries. In general, the results from the three different orientations agree to at least six significant digits. During the orientation check, it was found that several boundary conditions are imposed with the wrong sign. This causes some nodal quantities to be swapped and others to have the wrong signs. After taking this into account, there is no indication of orientation dependence from incorrect coding.

The through-thickness integration rules appear to be implemented correctly. The number of Gauss quadrature points has virtually no impact on the FE results. The answers are independent of the number of Gauss points used to at least the sixth significant digit. Results generated using two-point Gauss quadrature and the user defined integration rule agree to five significant digits or more. Steady-state results generated using two-point Gauss quadrature and trapezoidal integration with fifty points differ by less than 0.09% for flexural cases and even less (< 0.0001%) for the uni-axial loading cases.

The choice of hourglass stabilization method has little effect on the results for the load cases examined. The FE generated steady-state values obtained using the different hourglass methods deviate by less than 0.1% from one another.

The steady-state results from runs made using two-point Gauss quadrature and, as applicable, stiffness stabilization are compared to the previously identified reference solutions. Tables 4 and 5 contain the relative error from the reference solution values, defined as

$$\% \text{ difference} = 100 \times (\text{DYNA3D result} - \text{reference solution})/\text{reference solution} \quad (4)$$

for the quadrilateral and triangular shell element formulations, respectively. The FE values represent the average of both nodal quantities at the corresponding longitudinal location. Although the FE model contains only three quadrilateral or six triangular shell elements, the maximum difference for quadrilateral formulations is less than 6% for flexural loadings and even less for extensional loadings. The deviation is greater for triangular formulations, but this is expected since only some of the boundary conditions imposed are consistent with a triangular discretization. Based upon the previously discussed convergence study, the deviation from the reference solutions is due to a lack of discretization and, for triangular formulations, inconsistent boundary conditions, and not implementation error.

Table 4: *Percent Difference From Reference Solution – Quadrilateral Formulations*

CASE		*BD*	*BLT*	*BLTR*	*HL*	*MEM*	*Y*	*Y4*
1	u_i	0.0110	0.0110	0.0200	0.0110	0.0110	0.0110	0.0110
3	u_k	-5.1895	-2.7407	-5.1895	-2.7407	N/A	-4.7409	-5.1157
	ϕ_j	-1.7652	-0.0248	-1.7652	-0.0248	N/A	-1.4293	-1.7092
5	u_k	-1.6756	-0.0269	-1.6756	-0.0269	N/A	-1.2917	-1.6114
	ϕ_j	-0.9961	-0.0108	-0.9961	-0.0108	N/A	-0.7600	-0.9567
6	F_i	-0.0242	-0.0367	-0.0459	-0.0367	-0.0367	-0.0368	-0.0369
8	F_k	5.4678	2.7910	5.4544	2.7910	N/A	4.9605	5.3729
	M_j	5.4651	2.7883	5.4518	2.7883	N/A	4.9578	5.3702
	ϕ_j	3.6691	2.8437	3.6691	2.8437	N/A	3.5341	3.6476
10	M_j	0.9892	-0.0179	0.9764	-0.0179	N/A	0.7296	0.9355
	u_k	-0.6967	-0.0357	-0.6967	-0.0357	N/A	-0.5322	-0.6694

N/A – Not applicable

Table 5: *Percent Difference From Reference Solution – Triangular Formulations*

CASE		*BCIZ*	*C0*
1	u_i	0.0110	0.0110
3	u_k	-1.7904	-7.4321
	ϕ_j	-0.384	-4.1325
5	u_k	-0.1374	-4.1868
	ϕ_j	-2.0342	-1.6742
6	F_i	-0.0146	-0.0146
8	F_k	1.8565	8.1346
	M_j	1.8538	8.1317
	ϕ_j	1.4939	3.6986
10	M_j	-23.561	-11.888
	u_k	-20.981	-13.096

Steady-state results generated using trapezoidal integration with fifty points show excellent agreement with those generated using two-point Gauss quadrature. Neglecting quantities that achieve no steady-state values, the trapezoidal answers differ from the Gauss quadrature values by 0.083% for non-zero flexural related quantities and by less than 0.00003% for all other quantities - for all shell formulations. The difference in flexural quantities exactly matches the predicted difference. (For n equal 50, e_{mom} equals 0.083%.) Consequently, it appears that trapezoidal integration is functioning correctly.

7 CONCLUSIONS

A series of small-displacement, linear elastic, regression problems are developed to test the shell elements in DYNA3D. The problems explore all triangular and quadrilateral shell formulations, three through-thickness integration options, three hourglass stabilization methods, and the two alternative reference surface location available for the Hughes-Liu shell formulation. The problems utilize displacement/rotation- and force/moment-type boundary conditions to probe each of the active nodal degrees of freedom. Consequently, these problems are sensitive to any future modifications made to DYNA3D's present shell implementations.

While developing and testing the regression problems, the shell element implementation was, in part, verified as well as validated for modeling beam-like structures. The test problem results show that for all formulations the implementations are independent of shell element orientation, the through-thickness integration rules yield the correct results, and the elements respond correctly to imposed boundary conditions, i.e., no implementation deficiencies were identified. The structures simulated in the FE decks depict simple cantilever beams of constant cross section loaded at their tips in a variety of ways. Even with the crude discretization employed, the numerical results show good agreement with reference solution values.

8 REFERENCES

1. Lin, J.I., "DYNA3D: A Nonlinear, Explicit, Three-Dimensional Finite Element Code for Solid and Structural Mechanics, User Manual", Lawrence Livermore National Laboratory, UCRL-MA-107254, June 2005.

2. Beer, F.P. and Johnston, E.R., *Mechanics of Materials*, McGraw-Hill Book Company, New York, 1981.

3. Rathbun, H, "Beam and Truss Finite Element Verification for DYNA3D," Lawrence Livermore National Laboratory, UCRL-TR-232789, 2007.

4. Young, W.C., **Roark's Formulas for Stress and Strain**, 6-th ed., McGraw-Hill, New York, 348, 1989.